

# Signature of Mott-insulator transition with ultra-cold fermions in a one-dimensional optical lattice

Xia-Ji Liu<sup>1</sup>, Peter D. Drummond<sup>1</sup> and Hui Hu<sup>2,3</sup>

<sup>1</sup> *ARC Centre of Excellence for Quantum-Atom Optics, Department of Physics, University of Queensland, Brisbane, Queensland 4072, Australia*

<sup>2</sup> *NEST-INFM and Classe di Scienze, Scuola Normale Superiore, I-56126 Pisa, Italy*

<sup>3</sup> *Interdisciplinary Center of Theoretical Studies, Chinese Academy of Science, P. O. Box 2735, Beijing 100084, P. R. China*

(Dated: 23rd May 2019)

Using the exact Bethe ansatz solution of the Hubbard model and Luttinger liquid theory, we investigate the density profiles and collective modes of one-dimensional ultra-cold fermions confined in an optical lattice with a harmonic trapping potential. We determine the generic phase diagram in terms of a characteristic filling factor and a dimensionless coupling constant. The collective oscillations of the atomic mass density, a technique that is commonly used in experiments, provides a signature of the quantum phase transition from the metallic phase to the Mott-insulator phase. A detailed experimental implementation is proposed.

PACS numbers: 03.75.Ss, 03.75.Kk, 71.10.Pm, 71.30.+h

*Introduction.* — The Mott metal-insulator transition (MMIT) is a fundamental concept in strongly correlated many-body systems. Recent experiments with ultra-cold atomic gases in optical lattices are paving the way to explore such quantum phase transitions in a well-controlled manner. The MMIT with bosonic atoms has been demonstrated by Greiner *et al.* [1]. A demonstration with fermions has not yet been realized experimentally, although its realization is within reach of present-day techniques. In the fermionic case, the relevant theory is the widely studied Hubbard model. This is the simplest lattice model of interacting fermions, and is exactly soluble in one dimension.

A gas of spinless <sup>40</sup>K atoms in a parallel plane lattice has already been created by the LENS group, thanks to rapid progress in the cooling of fermions to temperatures below a micro-Kelvin. This demonstrated a non-interacting band insulator behavior [2, 3, 4] through the observation of dipole mode oscillations. An interacting gas of ultra-cold fermions with spin degrees of freedom in a one-dimensional lattice is also feasible, thus offering the possibility of observing the fermionic MMIT.

Motivated by this opportunity, we address the problem of how to detect the emergence of fermionic Mott-insulator phases in real experiments with ultra-cold atoms. With optical lattices, a harmonic potential is necessary to prevent the atoms from escaping, so that the Mott-insulator phase is restricted to an insulator domain at the center of the trap, and coexists with two compressible metallic wings. Therefore, the insulator phase cannot be characterized by a global compressibility as in the unconfined case. Rigol *et al.* [5] showed that a properly defined local compressibility exhibits critical behavior on approaching the boundary between the insulator domain and the metallic wings. But it is not clear how to measure a purely localized compressibility in a real experiment.

In this Letter we show that collective oscillations of the atomic mass density, an indicator of compressibility,

can be utilized to monitor the emergence of the Mott-insulator phase. We consider a zero temperature, one-dimensional Hubbard model with a harmonic potential, as a model of an ultra-cold spin-1/2 fermionic atomic cloud in a deep optical lattice with strong radial and weak axial confinement. Based on the exact Bethe ansatz solution of the homogeneous 1D Hubbard model [6], together with the local density approximation (LDA), we calculate the density profile of the cloud as functions of a characteristic filling factor and coupling constant. This leads to a generic phase diagram including a metallic phase and a Mott-insulator phase. We then investigate the collective density oscillations of the cloud in different phases using Luttinger liquid (LL) theory [7], which describes long wavelength hydrodynamic behaviour.

We find that in the metallic phase the collective oscillation is an overall motion that goes through all sites of the cloud. This quenches gradually towards the phase transition point, with the mode frequency decreasing monotonically to zero. After entering the Mott-insulator phase, the density oscillation revives, but is restricted to the compressible wings. The corresponding frequency increases rapidly. Therefore, a sharp dip appears in all collective mode frequencies in the vicinity of the phase boundary, giving a clear signature of the MMIT.

*Phase diagram.* — We consider the 1D Hubbard model [6], as a prototype for  $N$  ( $N/2 = N_{\uparrow} = N_{\downarrow}$ ) interacting fermions in deep optical lattices, with a Hamiltonian given by:

$$\mathcal{H}_0/t_h = u \sum_i n_{i\uparrow}n_{i\downarrow} - \sum_{i\sigma} (c_{i\sigma}^{\dagger}c_{i+1\sigma} + h.c.). \quad (1)$$

Here  $t_h$  and  $u$  ( $u > 0$ ) are the hopping parameter and the dimensionless on-site repulsion, respectively. The spin  $\sigma = \uparrow, \downarrow$  represents the different hyperfine states of fermions. The presence of an axial harmonic trap adds a

site dependent potential to the Hamiltonian so that:

$$\mathcal{H} = \mathcal{H}_0 + \sum_{i\sigma} \frac{m\omega_0^2}{2} d^2 i^2 n_{i\sigma}, \quad (2)$$

where  $\omega_0$  is the bare trapping frequency and  $d = \lambda/2$  is the lattice periodicity, while  $\lambda$  is the wavelength of standing waves used to create the 1D optical lattice. We describe the inhomogeneous gas, Eq. (2), within the LDA. This amounts to determining the chemical potential of the gas from the local equilibrium condition,

$$\mu = \mu_{\text{hom}}[n(x), u] + \frac{m\omega_0^2}{2} d^2 x^2. \quad (3)$$

We also impose a normalization condition,  $\sum_{i=-\infty}^{+\infty} n(i) = \int_{-\infty}^{+\infty} n(x) dx = N$ , using  $\mu_{\text{hom}}[n(x), u]$  as the chemical potential of a homogeneous system with a local filling factor  $n(x)$  ( $0 \leq n(x) \leq 2$ ) [10]. When using the LDA, we replace the site index  $i$  with a dimensionless variable  $x$ , in an approximation valid in the limit of a large lattice with a slowly varying trapping potential. Because of the optical lattice, the single-particle trapping frequency is renormalized to  $\omega_{\text{eff}} = (m/m^*)^{1/2} \omega_0$ , with an effective mass  $m^* = \hbar^2/(2d^2 t_h)$ . We also define a dimensionless frequency,  $\omega = \hbar\omega_{\text{eff}}/(2t_h)$ , with corresponding dimensionless time  $\tau = t\omega_{\text{eff}}/\omega$ .

To construct the phase diagram, it is useful to introduce two parameters:

- $\kappa = u^2/(16N\omega)$  is the interaction strength
- $\nu = 2\sqrt{N\omega}/\pi$  is the characteristic filling factor

We clarify the physical meanings of these parameters by considering two limiting cases.

(i) In the limit of a dilute Fermi cloud [ $n(i) \rightarrow 0$ ], the Hubbard model reduces to Yang's exactly solvable Fermi gas model. Therefore, the homogeneous chemical potential takes the form  $\mu_{\text{hom}}[n, u] = (2t_h)(\pi^2 n^2/8)\mu'_{\text{hom}}[u/(2n)]$  up to an irrelevant constant. The function  $\mu'_{\text{hom}}$  is obtained by solving a set of integral equations [8].

In terms of the dimensionless chemical potential  $\tilde{\mu} = 8\mu/(u^2 t_h)$  and the rescaled coordinate  $\tilde{x} = 4\omega x/u$ , the local equilibrium and normalization conditions can be re-expressed as:  $\pi^2/[2\gamma^2(\tilde{x})]\mu'_{\text{hom}}[\gamma(\tilde{x})] + \tilde{x}^2/2 = \tilde{\mu}$  and  $\int_{-\infty}^{+\infty} 2/\gamma(\tilde{x}) d\tilde{x} = 16N\omega/u^2$ , where  $\gamma(\tilde{x}) = u/[2n(\tilde{x})]$ . These equations indicate that the coupling strength is  $\kappa = u^2/(16N\omega)$ , where  $\kappa \ll 1$  corresponds to weak couplings and  $\kappa \gg 1$  is the strongly interacting regime.

(ii) In the non-interacting limit,  $\mu_{\text{hom}}[n, u=0] = -2t_h \cos(\pi n/2) \xrightarrow{n \rightarrow 0} 2t_h(-1 + \pi^2 n^2/8)$ . It is straightforward to show that the central number density is  $n(x=0) = 2\sqrt{N\omega}/\pi$ , which we define as the characteristic filling factor  $\nu$ .

Fig. 1 shows the central density  $n(x=0)$  as a function of  $\nu$  for three values of  $\kappa$ . We have identified five phases as explained in the figure caption. In the weak coupling

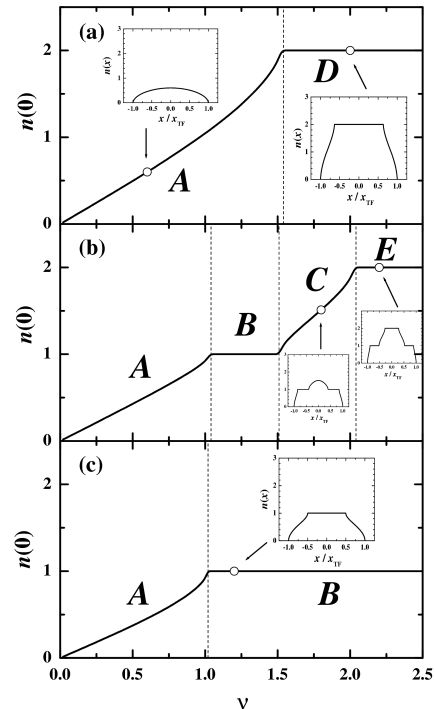


Figure 1: Central densities  $n(x=0)$  as a function of  $\nu$ , for three values of  $\kappa = 0.01$  (a), 1 (b), and 100 (c). The dashed lines divide the system into different phases and the corresponding typical density profiles are shown in insets. The different phases obtained can be classified as follows. A: a pure metallic phase, which always occurs in the wings. B: a single Mott insulator domain in the center. C: a metallic phase at the center surrounded with Mott insulator plateaus. D: a band insulator at the center with metallic wings outside. E: a band insulator at the trap center surrounded by metallic regions, in turn surrounded by Mott insulators.

limit ( $\kappa = 0.01$ ), an increase of the characteristic filling factor changes the cloud from a metal to a band insulator. In the strong coupling regime ( $\kappa = 100$ ), the cloud becomes a Mott insulator with increasing  $\nu$ . It is worth mentioning that the existence of traps leads to two new phases (C and E) that have no correspondence in the unconfined case. This occurs for the intermediate coupling regime with  $0.1 < \kappa < 10$ . An example is shown in Fig. 1b to illustrate the successive emergence of phases C and E as  $\nu$  increases.

We determine the phase diagram in Fig. 2 from the density profiles. We have plotted a dashed line to illustrate the crossover behavior from A to C, or D to E. On the left side of the dashed line there is no Mott insulator plateau. In Fig. 5 of Ref. [5], Rigol *et al.* also proposed a phase diagram. However, their incomplete phase diagram covers only the weak and intermediate interaction regimes of  $\kappa < 1.0$ .

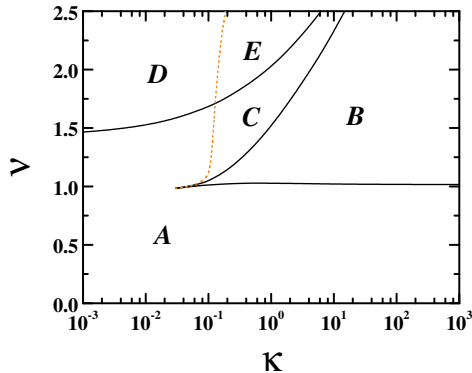


Figure 2: Phase diagram of one-dimensional confined Fermi gases in optical lattices. See also Fig. 5 in Ref. [5].

*Collective density oscillations.* — To detect experimentally the phase diagram (Fig. 2), we turn to investigate the collective density oscillations. We describe the low-energy dynamics of density fluctuations of metallic regions in each phase using the LL model of the 1D Fermi gas in optical lattices [7], where the Hamiltonian can be written as:

$$\mathcal{H}_{\text{LL}} = \sum_{\nu=\rho,\sigma} \int dx \frac{u_\nu(x)}{2} \left[ K_\nu(x) \Pi_\nu^2 + \frac{1}{K_\nu(x)} \left( \frac{\partial \phi_\nu}{\partial x} \right)^2 \right]. \quad (4)$$

Here  $u_\rho$  and  $u_\sigma$  are the density and spin velocities, respectively, and  $K_\rho$  and  $K_\sigma$  are the Luttinger exponents of long-wavelength correlation functions. These parameters in a spatially homogeneous gas can be calculated from the Bethe ansatz solution of the 1D Hubbard model [9, 10]. In the Hamiltonian, we have already used the LDA, *i.e.*,  $u_\nu(x) \equiv u_\nu(n(x))$  and  $K_\nu(x) \equiv K_\nu(n(x))$ . The canonical momenta  $\Pi_\nu$  are conjugate to the phases  $\phi_\nu$ , *i.e.*,  $[\phi_\nu(x), \Pi_\mu(x')] = i\delta_{\mu\nu}\delta(x-x')$ . Physically, the gradients of the phases  $\partial_x \phi_\nu(x)$  are proportional to the density (or spin density) fluctuations,  $\delta n_\nu(x) = -\partial_x \phi_\nu(x)$ , while the momenta  $\Pi_\nu(x)$  are proportional to the density (or spin density) currents,  $j_\nu(x) = u_\nu(x)K_\nu(x)\Pi_\nu(x)$ .

From this approximate Hamiltonian, we derive the hydrodynamic equation of motion:

$$\frac{\partial^2 \delta n_\nu}{\partial \tau^2} = \frac{\partial}{\partial x} \left[ u_\nu(x) K_\nu(x) \frac{\partial}{\partial x} \left( \frac{u_\nu(x)}{K_\nu(x)} \delta n_\nu \right) \right]. \quad (5)$$

Hereafter we focus on the readily observable density modes. We consider the  $n$ -th eigenmode with  $\delta n_\rho(x) \sim \delta n_\rho(x) \exp(i\omega_n \tau)$  and substitute it into Eq. (5). The resulting equation for  $\delta n_\rho(x)$  is solved using boundary conditions which require the current  $j_\rho(x)$  to vanish [11]. The details, together with the interesting question of spin-charge separation, will be presented elsewhere [12].

Fig. 3 shows the frequencies of the breathing mode and of the dipole mode at fixed values of  $\nu$  and of  $\kappa$ . For

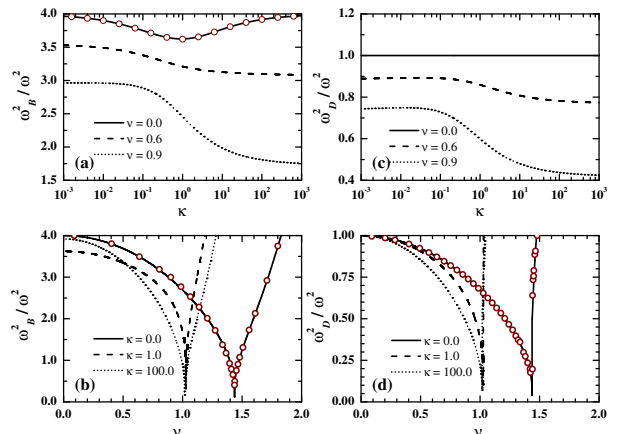


Figure 3: Frequencies of the breathing mode and of the dipole mode at fixed values of  $\nu$  (Figs. 3a and 3b) and of  $\kappa$  (Figs. 3c and 3d). The circles in (a) are the predictions of the sum-rule approach, while the circles in (b) and (d) are the results for the non-interacting Fermi gas, obtained by solving the semi-classical Boltzmann kinetic equations.

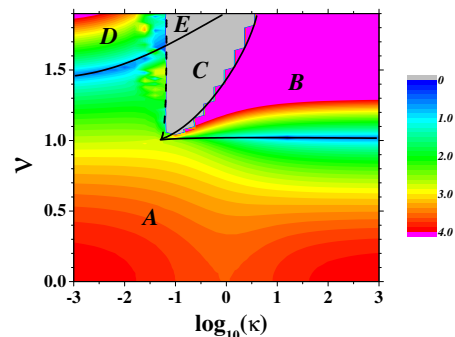


Figure 4: (color) The contour plot of the breathing mode frequency as functions of  $\nu$  and of  $\kappa$  (in a logarithmic scale). The breathing modes in phases C and E are not explored, with the unknown frequencies shown by gray. The regions with  $\omega_B^2/\omega_0^2 \geq 4$  have been displayed by magenta.

a constant value of  $\kappa$ , the remarkable feature shown in Figs. 3b and 3d is the appearance of a sharp dip at a particular value of the characteristic filling factor, which has been identified as the transition point from a metal to an insulator. On the left side of the transition point, the cloud is a pure metal and the density fluctuates at all sites. The decrease of the frequency with increasing  $\nu$  can be understood from the fact that in the homogeneous case the cloud has a sound-like spectrum, and the sound velocity  $u_\rho$  decreases as  $u_\rho \propto 1 - n$  on approaching the transition point at  $n = 1$ , due to the opening of the charge gap. For larger filling, an insulating domain forms at the center of the trap, in which the LL description

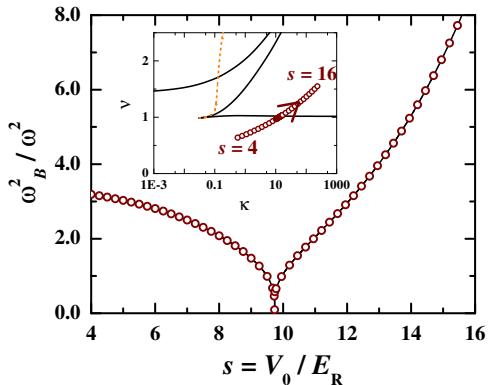


Figure 5: (color online) A proposed experimental scheme. The breathing mode frequency has been plotted as a function of the depth of the lattice potential for a gas of potassium atoms. Other parameters are described in the text. The inset shows the path in the phase diagram with increasing the depth of optical lattices.

breaks down. In response to a trap displacement, the center of mass will develop a quasi-static displacement in this case. Our theory is able to describe the *local* oscillations of the metallic wings around this new origin.

We have verified this expectation by using the semi-classical Boltzmann kinetic theory for a non-interacting cloud [4]. As  $\nu$  increases, the metallic wings shrink in size and become less compressible. Therefore the mode frequency rises after crossing the transition point. For better illustration we display in Fig. 4 a contour plot of breathing mode frequencies as functions of  $\nu$  and of  $\kappa$ . The blue regions with small mode frequency indicate a phase transition from a metal to a band insulator ( $A \rightarrow D$ ) or to a Mott insulator ( $A \rightarrow B$ ).

We have examined the validity of the LL theory for collective oscillations by using alternative methods in two limiting cases. In Fig. 3a the open circles are the prediction of  $m_3/m_1$  or  $m_1/m_{-1}$  sum-rules at  $\nu \rightarrow 0$  [13]. The excellent agreement shows that the LL theory is correct at low density. For a non-interacting gas at a *finite* filling factor, we calculate the mode frequency by solving the semi-classical Boltzmann kinetic equation [4]. As shown by open circles in Figs. 3b and 3d, this leads again to the same result obtained by the LL theory. However, the LL theory is less reliable for strongly interacting gases at large filling factors. This may slightly modify the mini-

um mode frequency.

*Experimental proposal.* — Finally we propose an experimental scheme following a recent experiment [14]. A 1D optical lattice is formed by the standing wave  $V_0(x) = sE_R \sin^2(\pi z/d)$  where  $sE_R = s\hbar^2\pi^2/(2md^2)$  is the recoil energy. For a deep lattice potential with  $s \gg 1$ , we approximate the Wannier function by the lowest harmonic oscillator state. This leads to a coupled expression for  $t_h$ ,  $u$  and  $\omega$ , in terms of the lattice periodicity  $d$ , lattice depth  $s$ , effective 1D scattering length  $a_{1D}$  and bare frequency  $\omega_0$ :  $t_h = \pi^2\hbar^2s(\pi^2/4 - 1)\exp(-\pi^2s^{1/2}/4)/(2md^2)$ ,  $u = -2d\sqrt{\pi/2}s^{1/4}\hbar^2/(t_hmd^2a_{1D})$ , and  $\omega = d^2(\pi^2/4 - 1)^{-1/2}s^{-1/2}\exp[\pi^2s^{1/2}/8]/(\pi a_{ho}^2)$ . Here  $a_{ho} = \sqrt{\hbar/(m\omega_0)}$ . Experimentally,  $a_{1D}$  is related to the 3D scattering length by  $a_{1D} = -(1/2\pi)^2s_{2d}^{-1/2}\lambda_{2d}^2/a_{3D}$ , where  $s_{2d}$  and  $\lambda_{2d}$  are the depth and the wavelength of the transverse standing waves.

As experimental parameters [14], we take  $N = 15$ ,  $\omega_0 = 2\pi \times 60$  Hz,  $2d = 854$  nm,  $\lambda_{2d} = 823$  nm, and  $s_{2d} = 27$ . For  $^{40}\text{K}$  atoms we shall use an inter-species interaction  $a_{3D} = +26a_B$ , where  $a_B = 0.529$  Å is the Bohr radius. The value of  $a_{3D}$  can also be tuned by a Feshbach resonance. We show the frequency of the breathing mode as a function of the depth  $s$  of the lattice potential in Fig. 5. Though the sharpness of the frequency dip may be weakened by finite temperatures or nonlinear effects due to (finite amplitude oscillations), it will signal the entrance into the Mott-insulator phase.

*Conclusions.* — In summary, we present a phase diagram for 1D confined fermions in an optical lattice. We show that the behavior of the frequencies of collective density modes is distinct in each phase. Therefore, the phase diagram can be detected unambiguously by measuring density oscillations. This provides a useful tool for locating the quantum phase transition from the metallic phase to the Mott-insulator phase. We expect that a similar sensitivity of the mode frequencies with respect to the phase will arise in higher dimensions. Furthermore, this signature could be applied as well to a gas of 1D bosons in an optical lattice, since the behavior of its low-energy excitations in the superfluid phase falls in the same universality class as the LL theory.

X.-J. L and P. D. D gratefully acknowledge support by the Australian Research Council. H. H was partially supported by INFM under the PRA-Photonmatter Programme.

- 
- [1] M. Greiner *et al.*, Nature (London) **415**, 39 (2002).  
 [2] L. Pezze, *et al.*, Phys. Rev. Lett. **93**, 120401 (2004).  
 [3] C. Hooley and J. Quintanilla, Phys. Rev. Lett. **93**, 080404 (2004).  
 [4] T. A. B. Kennedy, Phys. Rev. A **70**, 023603 (2004); X.-J.

- Liu and P. D. Drummond, unpublished.  
 [5] M. Rigol, *et al.*, Phys. Rev. Lett. **91**, 130403 (2003).  
 [6] E. H. Lieb and F. Y. Wu, Phys. Rev. Lett. **20**, 1445 (1968).  
 [7] A. Recati, *et al.*, Phys. Rev. Lett. **90**, 020401 (2003).

- [8] C. N. Yang, Phys. Rev. Lett. **19**, 1312 (1967).
- [9] H. J. Schulz, Phys. Rev. Lett. **64**, 2831 (1990).
- [10] C. F. Coll, Phys. Rev. B **9**, 2150 (1974).
- [11] R. Combescot and X. Leyronas, Phys. Rev. Lett. **89** , 190405 (2002).
- [12] X.-J. Liu, P. D. Drummond, and H. Hu, unpublished.
- [13] E. Lipparini and S. Stringari, Phys. Rep. **175**, 103 (1989).
- [14] B. Paredes *et al.*, Nature (London) **429**, 277 (2004).